DOI: *http://dx.doi.org/10.18502/cjn.v24i1.???*

Current Journal of Neurology

Original Paper

Curr J Neurol 2025; 24(1): 1-9

Histogram analysis of diffusion weighted magnetic resonance imaging for predicting isocitrate dehydrogenase 1 mutation status in brain gliomas

Received: 05 Sep. 2024
Accepted: 02 Nov. 2024

Fatemeh Shahedi[1], Shahrokh Naseri[1], Mahdi Momennezhad[1], Kazem Anvari[2], Babak Ganjeifar[3], Marzieh Maleki[3], Parvaneh Layegh[4], Masoumeh Gharib[5], Amin Ghaemmaghami[1], Hoda Zare[1,6]

[1] Medical Physics Research Center, Mashhad University of Medical Sciences, Mashhad, Iran
[2] Cancer Research Center, Mashhad University of Medical Sciences, Mashhad, Iran
[3] Department of Neurosurgery, Ghaem Hospital, Mashhad University of Medical Sciences, Mashhad, Iran
[4] Department of Radiology, School of Medicine, Mashhad University of Medical Sciences, Mashhad, Iran
[5] Department of Pathology, School of Medicine, Mashhad University of Medical Sciences, Mashhad, Iran
[6] Department of Medical Physics, School of Medicine, Mashhad University of Medical Sciences, Mashhad, Iran

Keywords
Diffusion Magnetic Resonance Imaging; Glioma; Isocitrate Dehydrogenase; Mutation; Brain

Abstract

Background: Gliomas are a major type of central nervous system (CNS) tumor. Accurate diagnosis of glioma grade and molecular subtype such as isocitrate dehydrogenase 1 (IDH1) mutation status remains a challenge as required invasive biopsy, which is limited by sampling bias and procedural risks. Quantitative analysis of functional magnetic resonance imaging (MRI), particularly apparent diffusion coefficient (ADC) maps, can serve as a non-invasive diagnostic tool for gliomas. However, using ADC values from different tumor regions may not accurately reflect the tumors' heterogeneous nature. This study aims to investigate the diagnostic accuracy of histogram features of ADC maps across the entire tumor volume in differentiating between low-grade gliomas (LGGs) and high-grade gliomas (HGGs), as well as IDH1-wildtype from IDH1-mutated tumors.

Methods: This cross-sectional study included 30 patients with glioma who were assessed prior to undergoing surgical resection.

How to cite this article: Shahedi F, Naseri S, Momennezhad M, Anvari K, Ganjeifar B, Maleki M, et al. Histogram analysis of diffusion weighted magnetic resonance imaging for predicting isocitrate dehydrogenase 1 mutation status in brain gliomas. Curr J Neurol 2025; 24(1): 1-9.

Corresponding Author: Hoda Zare
Email: zareh@mums.ac.ir

The whole tumor histogram parameters, including mean, minimum, median, maximum, 10th, 25th, 75th, and 90th percentiles, mode, standard deviation (SD), kurtosis, inhomogeneity, skewness, and entropy, were obtained from the ADC maps. Statistical analysis was conducted to clarify associations between ADC histogram parameters, grade, and IDH1 mutation status. The sensitivity was determined to evaluate the performance of each parameter.

Results: The analysis revealed that 10th percentile ADC (ADC10th) had the highest sensitivity (87.5%, P = 0.0423) for discriminating between glioma grades and IDH1 mutation status, respectively.

Conclusion: The whole-tumor ADC histogram-profiling indicates potential value for predicting glioma grades and IDH1 molecular subtypes. However, further validation is required before clinical adoption.

Introduction

Gliomas represent the most common form of primary central nervous system (CNS) cancer in adults. The World Health Organization (WHO) classified gliomas into low-grade (grade I and II) and high-grade (grade III and IV) gliomas based on histopathologic characteristics. The high-grade gliomas (HGGs) are more aggressive with a worse prognosis. The WHO 2021 also incorporated multiple molecular and genetic features, including isocitrate dehydrogenase 1 (IDH1), alpha-thalassemia/mental retardation syndrome X-linked (ATRX), and 1p/19q, into the diagnostic and classification framework for adult diffuse gliomas.[1] In this report, the IDH1 mutation status is one of the key prognostic markers for molecular classification and prognostication in adult diffuse gliomas. Accordingly, both low-grade gliomas (LGGs) and HGGs are separated into IDH1-wildtype and IDH1-mutant.[2] Previous studies have shown that IDH1-mutant gliomas are less aggressive and more radiosensitive than IDH1-wildtype gliomas.[3] ATRX also acts as a tumor suppressor, and its loss is associated with increased cancer aggressiveness. The codeletion of chromosomal arms 1p and 19q is almost characteristic of oligodendroglioma tumors.[4] An accurate determination of these biomarkers' status is necessary to plan treatment strategies. The current gold standard for determining these molecular features is invasive brain biopsy, which has limitation of sampling error due to tumor heterogeneity,[5] and some patients cannot undergo surgery due to age or proximity of tumor to functional regions of the brain.[6] The imaging features, particularly magnetic resonance imaging (MRI) (as preferred imaging modality for initial diagnostic of brain tumors), can be used as a powerful supplementary tool for non-invasive molecular diagnosis of gliomas. However, conventional structural MRI has limited ability to predict glioma grades or molecular subtypes due to partially overlapping of morphological features.[7] Physiological imaging techniques like diffusion-weighted MRI (DWI) provide information on the random Brownian motion of water molecules in tissue. A major strength of DWI is apparent diffusion coefficient (ADC) maps, which illustrate the diffusion magnitude of water molecules in cerebral tissue, offering insights into tissue microscopic architecture and cellularity.[8] Recent studies have explored ADC features to identify biomarkers for glioma classification, with some demonstrating ADC's ability to differentiate between ATRX-loss gliomas and 1p/19q codeleted gliomas.[9-11] Moreover, among these studies, the IDH1 mutation status as the first genetic driver event has been paid a strong clinical attention.[12] Several studies have demonstrated that decreased ADC values are distinctly observed in HGGs[13-15] and the majority of IDH-mutant gliomas.[16,17] However, others have reported that ADC maps cannot differentiate between IDH-wildtype and IDH-mutant, as well as LGGs or HGGs.[18-20] Depending on the degree of malignancy and IDH1 mutation status, gliomas are characterized by elevated intratumoral heterogeneity, including necrosis, edema, or vascular changes across different regions.[21] A significant factor contributing to this difference among studies is linked to the utilization of mean ADC values derived from the regions of interest (ROIs) within different parts of tumor volume, which may not accurately describe the tumor condition because of the inherent heterogeneous nature of gliomas. The traditional ADC map analysis is based on drawing a ROI on a specific area of tumor that may impact the ADC values and interobserver variability.[22] However, the histogram analysis of the whole-tumor quantified textural changes of the magnetic resonance (MR) images provides not only the quantitative accumulated metrics (mode, percentiles, minimum and maximum values), but also the distribution metrics [inhomogeneity, kurtosis, entropy, skewness, and standard deviation (SD)]. These metrics quantitatively reflect tissue variation across tumor, thus facilitating the assessment of tumor heterogeneity.[23]

The majority of past DWI research has focused mainly on the first-order ADC histogram parameters, including the mean, median, and percentiles. Few studies have examined both first- and second-order features such as skewness and entropy of the entire tumor ADC histogram profile which could better reflects tumor heterogeneity. Despite advancements in MRI techniques, there are no dependable imaging biomarkers for effective molecular classification, necessitating further research to discover new biomarkers. As far as we know, the comprehensive assessment of the diagnostic accuracy of mean, minimum, median, maximum, 10^{th}, 25^{th}, 75^{th}, and 90^{th} percentiles, mode, SD, kurtosis, inhomogeneity, skewness, and entropy ADC parameters for differentiation of LGGs and HGGs as well as IDH1-wildtype tumors from IDH1-mutated has not been reported in previous studies. This study aimed to assess the diagnostic accuracy of ADC histogram profiles extracted from the whole tumor to classify IDH1-wildtype tumors from IDH1-mutated ones and differentiate between LGGs and HGGs.

Materials and Methods

Patient selection: This cross-sectional study included participants diagnosed with glioma prior to their initial surgical resection at Ghaem Hospital affiliated to Mashhad University of Medical Sciences, Mashhad, Iran, between February and October 2024. Based on the MedCalc analysis, to get a large enough sample for the analysis to be significant at $P < 0.05$ and power of 0.8, a total of 30 patients with primary cerebral glioma were included in this study. Since the treatment affects the ADC values, to prevent incorrect interpretation of results, patients receiving anti-tumor treatment before MRI were excluded from the study. All MRIs were conducted less than 2 weeks prior to surgery. The definite grades and IDH1 mutational status were proved by biopsy and histopathologic assessment on the basis of the WHO classification criteria established in 2016. The written informed consent was also collected from all participants.

MRI protocol: In all participants, MRI was conducted with a 1.5T Ingenia MRI scanner (Philips Medical Systems, Eindhoven, Netherlands). The MRI protocol included axial T1-weighted (T1w) spin echo (SE) sequences [repetition time/echo time (TR/TE): 550 msec/ 8 msec, flip angle: 90, slice thickness: 5 mm, acquisition matrix: 256 × 186] pre and post contrast agent injection, an axial T2-weighted (T2w) turbo spin echo (TSE) sequence (TR/TE: 4230/91, slice thickness: 5 mm, flip angle: 150, acquisition matrix: 384 × 288), and an axial DWI sequence [multi-shot echo planar imaging (EPI) sequence, flip angle: 90, TR/TE: 4100/103, slice thickness: 5 mm, acquisition matrix: 210 × 210].

Histogram analysis of ADC volumes: The diffusion-weighted images, T1w images, and T2w images were extracted from the institutional picture archiving and communication system (PACS) workstation as DICOM files. The ADC maps together with the T2w images were co-registered to the corresponding T1w images through a rigid-body transformation in statistical parametric mapping (SPM12, University College London, London, UK). The borders of the whole tumors were manually drawn on every slice of detectable tumor in contrast-enhanced T1w MR images by a radiologist. In non-enhancing tumors, the hyperintense regions were drawn on T2w MR images. The entire tumors boundaries were applied to the corresponding ADC maps. To assess the tumors' characteristics, the ADC histogram profiles of the entire tumor volume were consecutively calculated using the in-house software program developed using MATLAB software (MathWorks Inc., Natick, MA, USA), providing the following set of features: mean, minimum, median, maximum, 10^{th} percentile (ADCp10), 25^{th} percentile (ADCp25), 75^{th} percentile (ADCp75), 90^{th} percentile (ADCp90), mode, SD, kurtosis (peakedness of the histogram), inhomogeneity, skewness (asymmetry of the histogram), and entropy (irregularity of image intensity). In order to assess intraobsever variability, tumor boundaries for eight randomly selected patients were redelineated by the radiologist after a pause of two weeks. ADC histogram parameters derived from first segmentation were compared with second segmentation using a Wilcoxon signed-rank test.

Histopathologic analysis: All tumor specimens were preserved in formaldehyde and embedded in paraffin for immunohistochemical analysis and histopathological diagnosis. The embedded samples were sectioned to a thickness of 3 µm and stained with hematoxylin and eosin (H&E). Immunohistochemistry was performed using specific antibodies targeting IDH1-R132H. IDH1 immunolabelling that produced intense cytoplasmic staining was considered as IDH1-mutant.

All statistical analyses were conducted using

the SPSS software package for Windows (version 16, SPSS Inc., Chicago, IL, USA). The normality of the parameters (Gaussian distribution) was assessed with the Shapiro-Wilk test. The comparison of normally-distributed ADC histogram metrics between HGGs and LGGs as well as IDH-mutant and wild-type gliomas was conducted with independent t-test. The non-normally-distributed parameters were assessed using the Mann-Whitney U test. To determine the most useful distribution characteristics, we analyzed the effect size of each using Cohen's d for normally-distributed parameters and effect size r for non-normally-distributed parameters. According to statistical conventions, Cohen's d is interpreted as follows: small ($d < 0.3$), medium ($d = 0.5$), large ($d > 0.8$), and extremely large ($d > 1$).[24] The statistical conventions regarding effect size r interpretation are: ($r = 0.1$-0.3) small effect, ($r = 0.3$-0.5) moderate effect, and ($r \geq 0.5$) large effect.[25] The 95% confidence interval (CI) based on the difference between two groups was also reported. Due to lack of a healthy control group, the performance of the investigated histogram features, in terms of discrimination of LGGs from HGGs and IDH1-mutated gliomas from IDH1-wildtype gliomas, was assessed using the calculation of sensitivity for histogram features that exhibited statistically significant differences in the comparative statistics. The outcomes with P-values less than 0.05 ($P < 0.05$) were deemed statistically significant.

Results

Participant demographics: The patients including 10 women and 20 men whose age ranged from 22 to 80 years, with an average age of 48 years old, were included in this study. Based on the histologic classification, 8 patients were diagnosed with LGGs (WHO II: n = 8) and 22 participants were identified with HGGs (WHO III: n = 9, WHO IV: n = 13). Mutations in the IDH1 gene were found in 8 out of 8 grade II gliomas, 8 out of 9 grade III gliomas, and 5 out of 13 grade IV gliomas. With the second segmentation, the P-value was found to be more than 0.05 for histogram parameters, which revealed the intraobserver consistency.

Comparison of ADC histogram features between LGGs and HGGs: Figure 1 demonstrates the ADC maps, the corresponding contrast-enhanced T1w and T2w MRI images of gliomas with WHO grade II, III, and IV, as well as the corresponding ADC histogram images plotted using MATLAB software.

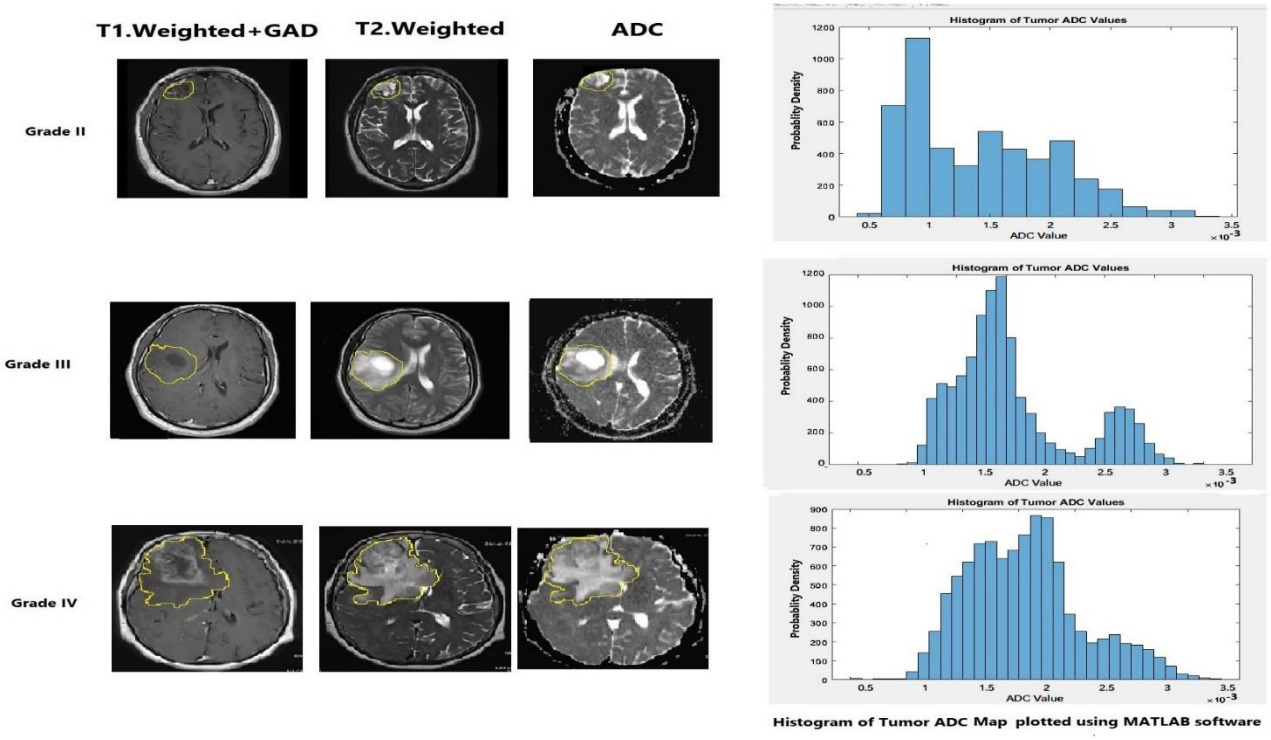

Figure 1. The T1-weighted (T1w) images after intravenous injection of a gadolinium-based contrast agent and the corresponding T2-weighted (T2w), apparent diffusion coefficient (ADC) maps, whole-tumor ADC histogram images plotted using MATLAB software in patients with World Health Organization (WHO) grade II, III, and IV glioma

The Shapiro-Wilk test indicated that ADC_{mode}, ADC_{mean}, $ADC_{minimum}$, $ADC_{maximum}$, ADCp10, ADCp25, ADCp75, ADCp90, ADC_{median}, homogeneity, ADC SD, and entropy (all Ps < 0.050) followed a Gaussian distribution. The skewness and kurtosis also indicated non-Gaussian distribution. Table 1 presents a summary of the findings from the comparative statistical analysis of ADC histogram data of all investigated patients. Statistically significant differences between LGGs and HGGs were found for the following ADC histogram features: median, minimum, ADCp10, ADCp25, kurtosis, and entropy (all Ps < 0.050). Specifically, the 10th percentile (P = 0.004, 95% CI = 50.34-88.66, Cohen's d = 2.01), 25th percentile (P = 0.049, 95% CI = 6.48-39.82, Cohen's d = 0.57), median (P = 0.007, 95% CI = 254.39-317.29, Cohen's d = 1.20), and minimum (P = 0.042, 95% CI = 13.10-64.34, Cohen's d = 0.78) were significantly lower in HGGs. The effect sizes indicate large effects for the minimum, median, and 10th percentile parameters, and a moderate effect for the 25th percentile in distinguishing HGGs from LGGs. The 95% CIs further support the statistical significance and impact of these parameters, as none include zero, suggesting a consistent and significant separation between the groups. Conversely, entropy (P = 0.008, 95% CI = -2.87, -1.69, Cohen's d = -2.40) and kurtosis (P = 0.023, 95% CI = -1.22, 4.88, r = -0.3) were found to be higher in HGGs. The CI for kurtosis includes zero, indicating uncertainty regarding the true effect of kurtosis in these populations. Based on the results, entropy (Cohen's d = -2.4) and the 10th percentile (Cohen's d = 2.01) were effective parameters for discriminating between HGGs and LGGs.

Comparison of ADC histogram features between IDH1-mutant and wild-type gliomas: Comparison of histograms from ADC maps between IDH1-mutated and IDH1-wildtype gliomas demonstrated statistically significant differences for the following features: minimum, maximum, ADCp10, inhomogeneity, and kurtosis. The complete results are presented in table 2. The histogram analyses showed significantly higher values for maximum (P = 0.0089, 95% CI = 18.4-262.2, Cohen's d = -0.9), inhomogeneity (P = 0.0002, 95% CI = 0.09-0.18, Cohen's d = -1.5), and kurtosis (P = 0.0344, 95% CI = 0.03-3.08, r = -0.3) in IDH1-wildtype tumors compared to IDH1-mutant gliomas. Additionally, lower values were found for ADCp10 (P = 0.0408, 95% CI = 15.21-44.27, Cohen's d = 1.1) and minimum (P = 0.0308, 95% CI = -25-32.42, Cohen's d = 0.63) in IDH1-wildtype tumors.

Table 1. Apparent diffusion coefficient (ADC) histogram parameters of whole tumoral tissue in low-grade gliomas (LGGs) and high-grade gliomas (HGGs)

Histogram features		LGG (mean ± SD)	HGG (mean ± SD)	95% CI	P	Effect size
First-order features	Minimum ($\times10^{-5}$ mm^2s^{-1})	59.21 ± 31.25	21.49 ± 22.17	(13.10, 64.34)	0.042	0.78[d]
	Maximum ($\times10^{-5}$ mm^2s^{-1})	273.01 ± 51.01	275.18 ± 51.88	(-110.00, 114.88)	0.970	-0.02[d]
	Mean ($\times10^{-5}$ mm^2s^{-1})	310.56 ± 34.81	146.97 ± 32.05	(-136.27, 432.77)	0.346	0.21[d]
	Median ($\times10^{-5}$ mm^2s^{-1})	372.98 ± 35.43	89.14 ± 33.13	(254.39, 317.29)	0.007	1.20[d]
	Mode ($\times10^{-5}$ mm^2s^{-1})	179.00 ± 45.58	118.00 ± 51.37	(19.80, 102.81)	0.345	0.30[d]
	ADCp10 ($\times10^{-5}$ mm^2s^{-1})	149.00 ± 19.63	81.00 ± 22.81	(50.34, 88.66)	0.004	2.01[d]
	ADCp25 ($\times10^{-5}$ mm^2s^{-1})	144.00 ± 53.60	125.00 ± 22.53	(6.48, 39.82)	0.049	0.57[d]
	ADCp75 ($\times10^{-5}$ mm^2s^{-1})	220.00 ± 43.11	151.00 ± 48.52	(-59.54, 84.78)	0.810	0.18[d]
	ADCp90 ($\times10^{-5}$ mm^2s^{-1})	270.00 ± 48.65	216.00 ± 51.32	(-149.00, 262.00)	0.598	0.35[d]
	SD ($\times10^{-5}$ mm^2s^{-1})	32.61 ± 14.68	42.31 ± 16.83	(-4.08, 23.48)	0.297	-0.51[d]
	Inhomogeneity	0.69 ± 0.08	0.62 ± 0.78	(-0.50, 0.64)	0.578	0.11[d]
Second-order features	Skewness[U]	0.57 ± 0.93	0.45 ± 0.81	(-0.48, 0.72)	0.679	0.06[r]
	Kurtosis[U]	2.25 ± 0.93	4.08 ± 4.12	(-1.22, 4.88)	0.023	-0.30[r]
	Entropy	2.90 ± 0.48	5.18 ± 0.76	(-2.87, -1.69)	0.008	-2.40

[d]Cohen's d parameter for effect size [small (d < 0.3), medium (d ~ 0.5), large (d > 0.8), and extremely large (d > 1) effect size]; [U]Parameters analyzed using Mann-Whitney U test [mean and standard deviation (SD) are reported for descriptive purposes]; [r]Non-parametric effect size, (r = 0.1-0.3) small effect, (r = 0.3-0.5) moderate effect, and (r ≥ 0.5) large effect

LGG: Low-grade glioma; HGG: High-grade glioma; ADC: Apparent diffusion coefficient; SD: Standard deviation; CI: Confidence interval

Table 2. Apparent diffusion coefficient (ADC) histogram parameters of whole tumoral tissue in isocitrate dehydrogenase 1 (IDH1)-mutant and IDH1-wild type gliomas

Histogram features		IDH1-mutant glioma (mean ± SD)	IDH1-wild type glioma (mean ± SD)	95% CI	P	Effect size
First-order features	Minimum ($\times10^{-5}$ mm^2s^{-1})	69.16 ± 21.84	56.30 ± 28.65	(-25.00, 32.42)	0.0308	0.63[d]
	Maximum ($\times10^{-5}$ mm^2s^{-1})	227.71 ± 48.23	263.56 ± 56.34	(18.40, 262.20)	0.0089	-0.90[d]
	Mean ($\times10^{-5}$ mm^2s^{-1})	190.06 ± 23.63	167.97 ± 34.85	(-177.66, 233.53)	0.7390	0.10[d]
	Median ($\times10^{-5}$ mm^2s^{-1})	197.95 ± 23.74	87.56 ± 32.48	(-144.00, 375.00)	0.3620	0.20[d]
	Mode ($\times10^{-5}$ mm^2s^{-1})	129.94 ± 34.22	156.15 ± 52.13	(-400.00, 340.00)	0.8800	-0.06[d]
	ADCp10 ($\times10^{-5}$ mm^2s^{-1})	104.87 ± 16.56	75.13 ± 20.62	(15.21, 44.27)	0.0408	1.10[d]
	ADCp25 ($\times10^{-5}$ mm^2s^{-1})	127.34 ± 21.32	95.46 ± 23.01	(-216.00, 279.00)	0.7990	0.07[d]
	ADCp75 ($\times10^{-5}$ mm^2s^{-1})	174.87 ± 22.63	156.77 ± 43.56	(-186.00, 240.00)	0.8660	0.07[d]
	ADCp90 ($\times10^{-5}$ mm^2s^{-1})	232.60 ± 31.24	231.22 ± 52.61	(-108.00, 104.00)	0.9770	0.01[d]
	SD ($\times10^{-5}$ mm^2s^{-1})	32.31 ± 8.13	43.51 ± 14.35	(-28.90, 6.44)	0.2160	-0.50[d]
	Inhomogeneity	0.61 ± 0.06	0.75 ± 0.05	(0.09, 0.18)	0.0002	-1.50[d]
Second-order features	Skewness[U]	0.56 ± 0.73	0.32 ± 0.75	(-0.07, 0.55)	0.1070	0.09[r]
	Kurtosis[U]	3.18 ± 1.13	4.55 ± 3.83	(0.03, 3.08)	0.0344	-0.30[r]
	Entropy	3.82 ± 0.35	6.12 ± 0.48	(-4.75, 0.14)	0.0671	-0.10[d]

[d]Cohen's d parameter for effect size [small (d < 0.3), medium (d ~ 0.5), large (d > 0.8), and extremely large (d > 1) effect size]; [U]Parameters analyzed using Mann-Whitney U test [mean and standard deviation (SD) are reported for descriptive purposes]; [r]Non-parametric effect size, (r = 0.1-0.3) small effect, (r = 0.3-0.5) moderate effect, and (r ≥ 0.5) large effect
ADC: Apparent diffusion coefficient; SD: Standard deviation; CI: Confidence interval; IDH-1: Isocitrate dehydrogenase 1

While the minimum parameter showed a notable difference with a moderate positive effect (Cohen's d = 0.63), its CI includes zero, indicating less certainty than other parameters. Inhomogeneity (Cohen's d = -1.5) was the most effective parameter for distinguishing IDH1-wildtype from IDH1-mutant gliomas.

Sensitivity analysis: The analysis revealed that the highest sensitivity for discriminating between LGGs and HGGs was detected for the ADC10th (87.5%, P = 0.0423), median (74.63%, P = 0.0438), and entropy (72.70%, P = 0.008), respectively. The ADC10th (88.10%, P = 0.0142), kurtosis (71.43%, P = 0.0433), and inhomogeneity (65.0%, P < 0.0001) also showed high sensitivity for distinguishing IDH1-mutated from IDH1-wildtype gliomas. Table 3 presents a comprehensive summary of the sensitivity analysis results.

Discussion

Histopathological and immunohistochemical analyses for diagnosing glioma grade and molecular subtype have limitations, such as sampling bias due to tumor heterogeneity, invasiveness, and delayed diagnoses which is unfavorable for pre-operative surgical planning.[26-28] Therefore, developing an effective, non-invasive method for predicting glioma genotyping is crucial for the treatment management. Gliomas exhibit heterogeneous microarchitecture and cellularity, which is not well represented by structural MR images.[7] This heterogeneity changes the diffusion pattern within a tumor, leading to different texture at the microscopic level in ADC MRI images, which cannot be visually assessed due to resolution limit. However, these textural changes can be quantified through histogram analysis.

This study evaluated whole-tumor ADC histogram profiles to identify reliable imaging biomarkers that distinguish between LGGs and HGGs, as well as those with and without IDH1 mutations. In this regard, our study demonstrated notably reduced values of first-order ADC histogram features, including the median, minimum, ADCp10, and ADCp25 in HGGs, aligning with findings from previous studies that showed lower ADC values correlated with reduced extracellular space and increased cellular proliferation, which restricts the diffusion of extracellular water molecules.[29,30]

Table 3. Sensitivity analysis of different apparent diffusion coefficient (ADC) histogram features for distinguishing low-grade gliomas (LGGs) and high-grade gliomas (HGGs) as well as isocitrate dehydrogenase 1 (IDH1)-mutated from IDH1-wildtype gliomas

Histogram features	Sensitivity (%)	P
Sensitivity analysis in differentiation of LGG and HGG		
Minimum ($\times10^{-5}$ mm^2s^{-1})	57.50	0.0378
Median ($\times10^{-5}$ mm^2s^{-1})	74.63	0.0438
ADCp10 ($\times10^{-5}$ mm^2s^{-1})	87.50	0.0423
ADCp25 ($\times10^{-5}$ mm^2s^{-1})	60.00	0.0436
Entropy	72.70	0.0080
Kurtosis	72.06	0.0035
Sensitivity analysis in differentiation of IDH1-mutant and IDH1-wildtype gliomas		
Maximum ($\times10^{-5}$ mm^2s^{-1})	41.15	0.0412
Minimum ($\times10^{-5}$ mm^2s^{-1})	40.50	0.0082
ADCp10 ($\times10^{-5}$ mm^2s^{-1})	88.10	0.0142
Inhomogeneity	65.00	< 0.0001
Kurtosis	71.43	0.0433

LGG: Low-grade glioma; HGG: High-grade glioma; ADC: Apparent diffusion coefficient; IDH-1: Isocitrate dehydrogenase 1

Lee et al. found lower ADC values for ADCp10 parameter in HGGs (P = 0.05), but their analysis used ROI measurements instead of whole-tumor profiling.[31] The whole-tumor histograms likely offer a more comprehensive evaluation of tumor heterogeneity, as indicated by the significant effect sizes for ADCp10 (P = 0.0043, CI = 50.34-88.66, Cohen's d = 2.01) in our study. Numerous studies indicate that lower ADC values serve as a negative prognostic biomarker in gliomas, correlating with poor survival rates.[32,33] In contrast, second-order parameters like entropy and kurtosis were significantly higher in HGGs (P < 0.05), reflecting increased microstructural randomness. These results are consistent with Kurokawa et al.[34] and Soliman et al.,[35] who reported elevated entropy (P = 0.001) and kurtosis (P = 0.004) in high-grade tumors, suggesting these metrics represent the chaotic architecture of aggressive gliomas. However, while entropy showed strong discriminative ability (Cohen's d = -2.4) between HGGs and LGGs, the CI for kurtosis included zero in our study, indicating uncertainty in its effect, possibly due to small sample size or data variability. The sensitivity analysis indicated that among the parameters with significant differences, ADC10th, median, and entropy had high sensitivity for identifying glioma grade, aligning with Ryu et al.[36] findings on entropy's role (P = 0.006) in assessing tumor heterogeneity. Conversely, Wang et al. found that tumoral inhomogeneity (P = 0.048) was effective in differentiating glioma grades.[37] This discrepancy may stem from the use of single ROI approach, compared to the whole tumor-volume approach used in this research. In addition to the morphological features, the IDH1 mutation is an important prognostic factor in patients with glioma. IDH1-mutated tumors are associated with more favorable individual outcomes and higher sensitivity to chemotherapy.[38] Regarding IDH1 mutation status, our study revealed higher values of maximum, inhomogeneity, and kurtosis, along with lower values of minimum and ADCp10 in IDH1-wildtype gliomas compared to IDH1-mutant tumors (P < 0.05). These findings align with reports by Liu et al.[39] and Lee et al.[40] who associated increased heterogeneity and reduced ADC values (minimum and ADCp10) with IDH1-wildtype gliomas, potentially reflecting greater cellularity, necrosis, and cystic degeneration. In our study, the minimum parameter showed less certainty compared to other parameters, as its CI included zero. In the current study, ADC10th, median, and entropy values demonstrated high sensitivity for distinguishing IDH1 mutation status.

This was in agreement with Liu et al. findings, which reported heterogeneity as one of the effective parameters in differentiating IDH1 mutation status in grade II and III gliomas.[39] However, the variations exist among studies regarding the reliability of different parameters, indicating a need for further investigation. For example, Gihr et al.[41] reported the entropy, while Lee et al.[40] reported the mean of ADC maps as an effective parameter in distinguishing IDH1 mutation status. The presented ADC histogram analysis highlights the likely potential of some parameters to differentiate glioma grades and

IDH1 mutation status. The non-invasive differentiation of grade and IDH1 mutation status could guide preoperative planning, and inform personalized treatment strategies, since IDH1-wildtype gliomas are less responsive to radiotherapy and chemotherapy.[3] By providing these insights preoperatively, whole-tumor ADC profiling could optimize therapeutic decision-making, ultimately improving patient outcomes. However, this study alone cannot fully validate the meaningfulness of these features, but it indicates the potential value of this imaging biomarker.

Our research has several limitations, including a relatively small sample size, a single-center study design, and the potential for selection bias. We utilized data exclusively from 1.5T MRI systems, which can result in decreased signal-to-noise ratios and consequently less spatial detail compared to higher field strengths. While the study focuses on imaging-derived features, other clinical variables that could influence IDH1 mutation status and glioma grade were not included in the statistical model. Additionally, the use of a manual segmentation method to delineate tumor boundaries and the assessment of intraobserver variability in relatively small number of patients may affect reproducibility. Further multi-center studies with a larger number of cases regarding integration of ADC histogram analysis with other advanced imaging modalities along with multivariable models considering additional factors affecting glioma grade and IDH1 mutation status could further refine diagnostic accuracy of histogram parameters and improve the features' reliability.

Conclusion

Whole-tumor histogram-derived ADC profiles provide various significant parameters, which indicate potential value for predicting glioma grades and IDH1 molecular subtypes. However, further investigations are required to validate the diagnostic performance of these parameters before clinical application.

Conflict of Interests

The authors declare no conflict of interest in this study.

Acknowledgments

We would like to express our sincere gratitude to Dr. Ganji for her guidance and technical support.

This study was supported by Mashhad University of Medical Sciences (grant no. 4020997). This study was also approved by the Institutional Review Board (IRB) of Mashhad University of Medical Sciences (IR.MUMS.MED.REC.1402.388) and followed the tenets of the Declaration of Helsinki.

References

1. Torp SH, Solheim O, Skjulsvik AJ. The WHO 2021 Classification of Central Nervous System tumours: a practical update on what neurosurgeons need to know—a minireview. Acta Neurochir 2022; 164(9): 2453-64.
2. Weller M, Felsberg J, Hentschel B, Gramatzki D, Kubon N, Wolter M, et al. Improved prognostic stratification of patients with isocitrate dehydrogenase-mutant astrocytoma. Acta Neuropathol 2024; 147(1): 11.
3. Yin N, Xie T, Zhang H, Chen J, Yu J, Liu F. IDH1-R132H mutation radiosensitizes U87MG glioma cells via epigenetic downregulation of TIGAR. Oncol Lett 2020; 19(2): 1322-30.
4. Koschmann C, Calinescu AA, Nunez FJ, Mackay A, Fazal-Salom J, Thomas D, et al. ATRX loss promotes tumor growth and impairs nonhomologous end joining DNA repair in glioma. Sci Transl Med 2016; 8(328): 328ra28.
5. Setyawan NH, Choridah L, Nugroho HA, Malueka RG, Dwianingsih EK. Beyond invasive biopsies: using VASARI MRI features to predict grade and molecular parameters in gliomas. Cancer Imaging 2024; 24(1): 3.
6. Davidson C, Woodford S, Valle D, Parker G, Derias A-M, Copley C, et al. Diffuse intrinsic pontine gliomas in pediatric patients: management updates. Egypt J Neurosurg 2023; 38(1): 64.
7. Kang XW, Xi YB, Liu TT, Wang N, Zhu YQ, Wang XR, et al. Grading of Glioma: combined diagnostic value of amide proton transfer weighted, arterial spin labeling and diffusion weighted magnetic resonance imaging. BMC Med Imaging 2020; 20(1): 50.
8. Le Bihan D. Apparent diffusion coefficient and beyond: what diffusion MR imaging can tell us about tissue structure. Radiology 2013; 268(2): 318-22.
9. Yang X, Hu C, Xing Z, Lin Y, Su Y, Wang X, et al. Prediction of Ki-67 labeling index, ATRX mutation, and MGMT promoter methylation status in IDH-mutant astrocytoma by morphological MRI, SWI, DWI, and DSC-PWI. Eur Radiol 2023; 33(10): 7003-14.
10. Ren Y, Zhang X, Rui W, Pang H, Qiu T, Wang J, et al. Noninvasive Prediction of IDH1 Mutation and ATRX Expression Loss in Low-Grade Gliomas Using Multiparametric MR Radiomic Features. J Magn Reson Imaging 2019; 49(3): 808-17.
11. Yang X, Lin Y, Xing Z, She D, Su Y, Cao D. Predicting 1p/19q codeletion status using diffusion-, susceptibility-, perfusion-weighted, and conventional MRI in IDH-mutant lower-grade gliomas. Acta Radiol 2021; 62(12): 1657-65.
12. Park JW, Kwak J, Kim KW, Jung S, Nam CH, Kim HJ, et al. IDH-mutant gliomas arise from glial progenitor cells harboring the initial driver mutation. bioRxiv 2024. [Preprint].
13. Momeni F, Abedi-Firouzjah R, Farshidfar Z, Taleinezhad N, Ansari L, Razmkon A, et al. Differentiating Between Low- and High-grade Glioma Tumors Measuring Apparent Diffusion Coefficient Values in Various Regions of the Brain. Oman Med J 2021; 36(2): e251.
14. Phuttharak W, Thammaroj J, Wara-Asawapati S, Panpeng K. Grading Gliomas Capability: Comparison between Visual Assessment and Apparent Diffusion Coefficient (ADC) Value Measurement on Diffusion-Weighted Imaging (DWI). Asian Pac J Cancer Prev 2020; 21(2): 385-90.

15. Agarwal A, Kanekar S, Sabat S, Bathla G. Value of quantitative apparent diffusion coefficients in differentiating low-grade gliomas from mixed neuronal-glial tumors. World Neurosurg X 2023; 18: 100159.
16. Thust SC, Hassanein S, Bisdas S, Rees JH, Hyare H, Maynard JA, et al. Apparent diffusion coefficient for molecular subtyping of non-gadolinium-enhancing WHO grade II/III glioma: volumetric segmentation versus two-dimensional region of interest analysis. Eur Radiol 2018; 28(9): 3779-88.
17. Du N, Zhou X, Mao R, Shu W, Xiao L, Ye Y, et al. Preoperative and Noninvasive Prediction of Gliomas Histopathological Grades and IDH Molecular Types Using Multiple MRI Characteristics. Front Oncol 2022; 12: 873839.
18. Wang Y, Fushimi Y, Arakawa Y, Shimizu Y, Sano K, Sakata A, et al. Evaluation of isocitrate dehydrogenase mutation in 2021 world health organization classification grade 3 and 4 glioma adult-type diffuse gliomas with 18F-fluoromisonidazole PET. Jpn J Radiol 2023; 41(11): 1255-64.
19. Brunberg JA, Chenevert TL, McKeever PE, Ross DA, Junck LR, Muraszko KM, et al. In vivo MR determination of water diffusion coefficients and diffusion anisotropy: correlation with structural alteration in gliomas of the cerebral hemispheres. AJNR Am J Neuroradiol 1995; 16(2): 361-71.
20. Rollin N, Guyotat J, Streichenberger N, Honnorat J, Tran Minh VA, Cotton F. Clinical relevance of diffusion and perfusion magnetic resonance imaging in assessing intra-axial brain tumors. Neuroradiology 2006; 48(3): 150-9.
21. Kashyap A, Rapsomaniki MA, Barros V, Fomitcheva-Khartchenko A, Martinelli AL, Rodriguez AF, et al. Quantification of tumor heterogeneity: from data acquisition to metric generation. Trends Biotechnol 2022; 40(6): 647-76.
22. Bilgili Y, Unal B. Effect of region of interest on interobserver variance in apparent diffusion coefficient measures. AJNR Am J Neuroradiol 2004; 25(1): 108-11.
23. Just N. Improving tumour heterogeneity MRI assessment with histograms. Br J Cancer 2014; 111(12): 2205-13.
24. Shankar JJ, Bata A, Ritchie K, Hebb A, Walling S. Normalized Apparent Diffusion Coefficient in the Prognostication of Patients with Glioblastoma Multiforme. Can J Neurol Sci 2016; 43(1): 127-33.
25. Elsayir A. Computation and interpretation of effect size in significance test. International Refereed Journal of Engineering and Science 2012; 1(4): 27-32.
26. Gilson P, Merlin JL, Harlé A. Deciphering Tumour Heterogeneity: From Tissue to Liquid Biopsy. Cancers (Basel) 2022; 14(6): 1384.
27. Guedes F, Henriques VM, Torrão FL, Haikal NP, Sanches GE, Barbosa DAN, et al. When biopsy goes wrong: a case series of misdiagnoses and complications from biopsies of masses of unknown origin potentially originating from a peripheral nerve. J Neurosurg 2023; 140(2): 480-8.
28. Patel SH, Bansal AG, Young EB, Batchala PP, Patrie JT, Lopes MB, et al. Extent of Surgical Resection in Lower-Grade Gliomas: Differential Impact Based on Molecular Subtype. AJNR Am J Neuroradiol 2019; 40(7): 1149-55.
29. Würtemberger U, Diebold M, Rau A, Akgün V, Becker L, Beck J, et al. Advanced diffusion imaging reveals microstructural characteristics of primary CNS lymphoma, allowing differentiation from glioblastoma. Neurooncol Adv 2024; 6(1): vdae093.
30. Boss MA, Malyarenko D, Partridge S, Obuchowski N, Shukla-Dave A, Winfield JM, et al. The QIBA Profile for Diffusion-Weighted MRI: Apparent Diffusion Coefficient as a Quantitative Imaging Biomarker. Radiology 2024; 313(1): e233055.
31. Lee J, Choi SH, Kim JH, Sohn CH, Lee S, Jeong J. Glioma grading using apparent diffusion coefficient map: application of histogram analysis based on automatic segmentation. NMR Biomed 2014; 27(9): 1046-52.
32. Bušić M, Rumboldt Z, Čerina D, Bušić Ž, Dolić K. Prognostic Value of Apparent Diffusion Coefficient (ADC) in Patients with Diffuse Gliomas. Cancers (Basel) 2024; 16(4): 681.
33. Zulfiqar M, Yousem DM, Lai H. ADC values and prognosis of malignant astrocytomas: does lower ADC predict a worse prognosis independent of grade of tumor?--a meta-analysis. AJR Am J Roentgenol 2013; 200(3): 624-9.
34. Kurokawa R, Hagiwara A, Kurokawa M, Ellingson BM, Baba A, Moritani T. Diffusion histogram profiles predict molecular features of grade 4 in histologically lower-grade adult diffuse gliomas following WHO classification 2021. Eur Radiol 2024; 34(2): 1367-75.
35. Soliman RK, Essa AA, Elhakeem AA, Gamal SA, Zaitoun MM. Texture analysis of apparent diffusion coefficient (ADC) map for glioma grading: Analysis of whole tumoral and peri-tumoral tissue. Diagn Interv Imaging 2021; 102(5): 287-95.
36. Ryu YJ, Choi SH, Park SJ, Yun TJ, Kim JH, Sohn CH. Glioma: application of whole-tumor texture analysis of diffusion-weighted imaging for the evaluation of tumor heterogeneity. PLoS One 2014; 9(9): e108335.
37. Wang S, Meng M, Zhang X, Wu C, Wang R, Wu J, et al. Texture analysis of diffusion weighted imaging for the evaluation of glioma heterogeneity based on different regions of interest. Oncol Lett 2018; 15(5): 7297-304.
38. Huang Y-R, Fan H-Q, Kuang Y-Y, Wang P, Lu S. The Relationship Between the Molecular Phenotypes of Brain Gliomas and the Imaging Features and Sensitivity of Radiotherapy and Chemotherapy. Clin Oncol 2024; 36(9): 541-51.
39. Liu D, Gao SX, Liao HF, Xu JM, Wen M. A Comparative Study of 2 Different Segmentation Methods of ADC Histogram for Differentiation Genetic Subtypes in Lower-Grade Diffuse Gliomas. Biomed Res Int 2020; 2020: 9549361.
40. Lee S, Choi SH, Ryoo I, Yoon TJ, Kim TM, Lee SH, et al. Evaluation of the microenvironmental heterogeneity in high-grade gliomas with IDH1/2 gene mutation using histogram analysis of diffusion-weighted imaging and dynamic-susceptibility contrast perfusion imaging. J Neurooncol 2015; 121(1): 141-50.
41. Gihr GA, Horvath-Rizea D, Hekeler E, Ganslandt O, Henkes H, Hoffmann KT, et al. Histogram Analysis of Diffusion Weighted Imaging in Low-Grade Gliomas: in vivo Characterization of Tumor Architecture and Corresponding Neuropathology. Front Oncol 2020; 10: 206.